

High dynamic exponents in vortex glass transitions: Dependence of critical scaling on the electric-field range

Patrick Voss-de Haan, Gerhard Jakob, and Hermann Adrian

Institut für Physik, Johannes Gutenberg-Universität Mainz, D-55099 Mainz, Germany

(Received 10 May 1999; revised manuscript received 9 July 1999)

We measured the dynamic response of the vortex system near the glass transition over an extremely wide electric-field range. Measurement bridges of 0.1-m length patterned from high quality $\text{YBa}_2\text{Cu}_3\text{O}_7$ films allowed the recording of current-voltage (I - V) curves from 1 V/m down to 10^{-8} V/m. We achieved excellent scaling of the I - V curves. The scaling is corroborated by the analysis of the resistive transitions and the crossover current J_0^+ which limits the critical region of the phase transition. While our results confirm the qualitative characteristics of a vortex glass phase transition, they yield an increased dynamic critical exponent at all magnetic fields. We also found a considerable dependence of the vortex glass scaling on the electric-field range probed. [S0163-1829(99)00541-X]

I. INTRODUCTION

Since the prediction of a vortex glass (VG) phase by Fisher, Fisher, and Huse^{1,2} (FFH) there has been a strong experimental effort to investigate the fluid to glass transition as well as the glass phase itself via transport³⁻⁸ and magnetization⁹ measurements. While the VG theory has been supported by various experiments reporting glass phases in $\text{YBa}_2\text{Cu}_3\text{O}_7$ (YBCO) and universal characteristic exponents for the transitions, there is still no clear agreement between theory and experiments. Recent results have shown a magnetic-field dependence of the critical exponents for $\mu_0 H < 0.05$ T.⁶ Also, in a combined transport-magnetization measurement a deviation from VG behavior was reported at very low electric fields,¹⁰ once more raising the question whether there is a truly superconducting phase ($\rho_{lin} \equiv \lim_{J \rightarrow 0} E/J \equiv 0$) for finite temperatures. Concerning the analysis of a VG transition it has been emphasized repeatedly in experimental as well as theoretical works that a restricted experimental window may generally result in misleading conclusions.^{3,11-14} Yet, current-voltage characteristics (CVC) obtained in transport measurements have typically covered no more than an electric-field range from 1 V/m down to only 10^{-5} V/m, whereas CVC's extracted from magnetization measurements usually have been limited to regimes between 10^{-6} and 10^{-11} V/m. We demonstrate by transport measurements on YBCO films that the measurement window strongly influences the analysis of CVC's. Parameters from a wider range (e.g., for the dynamic exponent $6 \leq z \leq 9$) yield an apparently equally satisfactory scaling for restricted measurement windows; however, if lower electric fields are included one observes a reduction of this scaling parameter range. The larger window accessible in our experiment reveals a somewhat decreased glass temperature T_g and more importantly a dynamic exponent z considerably higher than previously reported.

II. THE VORTEX GLASS MODEL

FFH considered a second-order phase transition occurring at T_g which is characterized by a diverging coherence length $\xi_g \propto |T - T_g|^{-\nu}$ and coherence time $\tau \propto \xi_g^z$, with static and dynamic exponents ν and z , respectively.² Electric field E

and current density J can be expressed as powers of these terms resulting in a scaling relation

$$E = J \xi_g^{d-2-z} \tilde{E}_{\pm}(J \xi_g^{d-1} \phi_0 / k_B T), \quad (1)$$

where \tilde{E}_{\pm} are universal scaling functions and $d=3$ is the dimensionality of the system. Accordingly, for a glass transition all I - V curves should collapse onto two common branches above (+) and below (-) T_g if the scaled quantities $(E/J)_{sc} \equiv (E/J) / |1 - T/T_g|^{\nu(z-d+2)}$ and $J_{sc} \equiv (J/T) / |1 - T/T_g|^{\nu(d-1)}$ are used. For temperatures $T < T_g$ the electric field decreases exponentially with the driving current $E \propto J \exp[-(J_0/J)^\mu]$. In a double logarithmic plot this will result in a negative curvature, which is commonly used to identify the glass region. If the current density exceeds a crossover current J_0^- the electric field is expected to approach asymptotically a power-law dependence. The I - V curve at T_g , separating the glassy regime of negative curvature from the fluid, should give a power-law dependence over the entire current range

$$E \propto J^{(z+1)/(d-1)}. \quad (2)$$

For temperatures $T > T_g$ one finds

$$\rho_{lin} \propto (T - T_g)^{\nu(z-d+2)}, \quad (3)$$

visible as linear CVC's at low current densities with an upturn at a crossover current J_0^+ , above which the I - V curves asymptotically approach the power-law dependence of the glass line. The crossover current vanishes as $J_0^+ \propto (T - T_g)^{\nu(d-1)}$. Combined with Eq. (3) this yields the crossover electric field

$$E_0^+ \propto (J_0^+)^{(z+1)/(d-1)}. \quad (4)$$

Thus in a double logarithmic plot of the CVC's the line connecting the crossover points of the various I - V isotherms is parallel to the I - V isotherm at the glass temperature with a slope of $(z+1)/(d-1)$. Above a fluid temperature T^* the linear resistivity [Eq. (3)] will be cut off due to the onset of free flux flow. This region can be observed in CVC's as well as in resistive transitions $\rho(T)$,¹⁵ and must therefore be excluded from the actual vortex glass analysis.

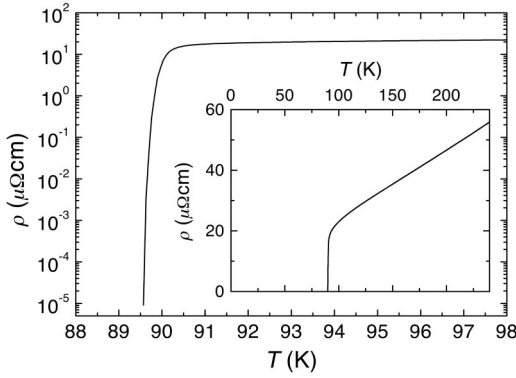


FIG. 1. Resistive transition of sample Y121. The inset gives the linear plot of the temperature dependence of the resistivity with $T_{c,midpoint} = 90.0$ K and a normal-state resistivity $\rho_{100\text{ K}} = 23 \mu\Omega\text{ cm}$. More importantly, the extremely narrow transition for a measurement bridge of this length becomes apparent in the logarithmic plot yielding a straight drop in resistance exceeding six orders of magnitude within 0.5 K.

The main problem in the analysis of CVC's in a double logarithmic plot is the comparatively small difference between I - V lines just above and below T_g which both display an asymptotic power-law behavior above J_0^\pm and—for limited intervals in the electric field—will appear as straight lines as expected for T_g only. Also, the onset of free flux flow at high electric fields results in a downward curvature for all I - V lines independent of any glass phase. Therefore, in order to investigate a VG phase, a large voltage window must be situated well below free flux flow and extend to very low electric fields.

III. SAMPLE PREPARATION AND EXPERIMENTAL PROCEDURE

In our experiment several YBCO thin films have been prepared by high-pressure dc-sputtering onto (001) SrTiO₃ substrates ($10 \times 10 \text{ mm}^2$), two of which were chosen due to their excellent homogeneity, high transition temperature, and small transition width as determined by inductive measurements before patterning. The samples have a thickness of about 400 nm and show excellent epitaxial c -axis oriented growth with typical rocking curve widths below 0.3° . A measurement bridge of $50\text{-}\mu\text{m}$ width with gold contact pads was prepared by photolithography and wet chemical etching. The bridge with a spiral shape and a length of 109 mm ($\mu_0 H_{self} < 1 \text{ mT}$ at J_{max}) allows the measurement of extremely low electric fields with a conventional nanovoltmeter. The transport measurements were carried out in a 6 T magnet cryostat with a temperature stability better than 0.05 K and a magnetic-field direction parallel to the c axis of the film. CVC's and resistive transitions were measured using rectangular current pulses of 1 s duration for each data point. Presented in Fig. 1 is the zero-field resistive transition of sample Y121, displaying a $T_{c,midpoint} = 90.0$ K, a normal-state resistivity $\rho_{100\text{ K}} = 23 \mu\Omega\text{ cm}$, and a very narrow transition width. The logarithmic plot reveals a straight drop in resistance ending below $10^{-5} \mu\Omega\text{ cm}$ and exceeding six orders of magnitude within 0.5 K. Thus T_c variations or other inhomogeneities due to poor sample quality will not obscure intrinsic properties. Here we present the data for Y121; the

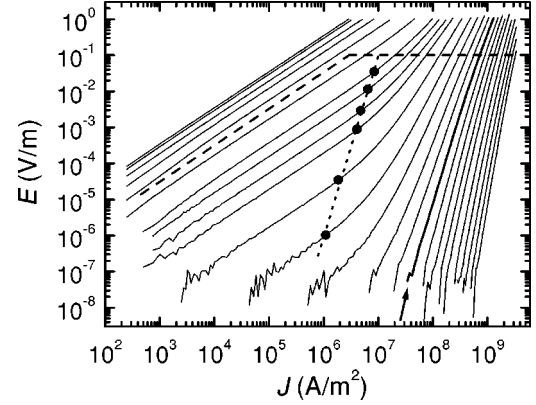


FIG. 2. The I - V curves of sample Y121 in an external field of 1.0 T for $91 \leq T \leq 80.5$ K. The I - V glass line at $T_g = 84.6$ K (arrow) and the location of the crossover $E_0^+(J_0^+)$ for all accessible temperatures (solid dots) display an identical slope. (Dashed lines indicate the onset of free flux flow relevant for the scaling in Fig. 3.)

other sample, Y151 with $T_c = 90.5$ K and a transition width of 1 K, shows the same results for resistive transitions and CVC's.

IV. EXPERIMENTAL RESULTS

A. The I - V glass line and the crossover current

Shown in Fig. 2 are CVC's taken at $\mu_0 H = 1.0$ T between $91.0 > T > 80.5$ K. The accessible electric-field range extends from 1 V/m to below 10^{-8} V/m. One can identify the characteristic regions of CVC's typical for YBCO films: For temperatures above 85.8 K the isotherms have a slope of 1 at low current densities and turn into an asymptotic power-law dependence above the crossover current J_0^+ resulting in a positive curvature. The I - V line at 84.6 K most closely follows a power-law behavior with a constant slope extending over more than five decades of the electric field. Below this temperature the isotherms show a negative curvature as to be expected for a VG state. However, for all applied magnetic fields (0.03–1.0 T) some I - V lines above T_g show both, a positive curvature at low current densities and negative curvature at high current densities. The latter is due to the onset of free flux flow but could easily be mistaken for the glassy phase or obstruct a scaling analysis. Excluding the data of this region ($E \geq 0.1$ V/m) from an analysis we can identify in all CVC's a single I - V line at the approximate T_g which separates the regions of positive and negative curvature. According to Eq. (2), its slope $s = (z+1)/(d-1)$ yields the dynamic exponent, z . For 1.0 T one observes $s = 5.01$ and $z = 9.0$ which is considerably larger than previously reported values for YBCO.^{3–8} The complete data for all magnetic fields are compiled in Table I along with the parameters extracted from J_0^+ , the glass scaling, and the Vogel-Fulcher analysis.

In order to extract $E_0^+(J_0^+)$ from the CVC's according to Eq. (4) we define the crossover of the I - V lines as the point for which $\rho(J) = 1.1 \rho_{lin}$. One observes a power-law dependence throughout the entire measurement window as indicated by the dotted line in Fig. 2. Its slope of 5.04 and the extracted dynamic exponent of $z = 9.1$ agree very well with that of the actual I - V glass line. Plotting $J_0^+(T)$ vs $T - T_g^3$ or $\xi^{(-1/\nu)}$ vs $T - T_g$ confirms this result and the absence of a length scale dependent cutoff.

TABLE I. T_g , T^* , and critical exponents, z and ν , resulting from glass line, J_0^+ , scaling, and Vogel-Fulcher analyses.

$\mu_0 H$ (T)	I-V glass line		$E_0^+(J_0^+)$		Glass scaling analysis				Vogel-Fulcher analysis		
	T_g (K)	z	z	T_g (K)	T^* (K)	z	ν	$\nu(z-1)$	T_g (K)	T^* (K)	$\nu(z-1)$
0.03	89.5(1)	11.1(8)	11.4(5)	89.50(10)	90.1(2)	11.2(3)	1.25(5)	12.75	89.4(4)	90.0(3)	11.3(9)
0.10	88.6(1)	11.2(6)	10.0(4)	88.65(10)	89.8(2)	10.4(3)	1.45(5)	13.63	88.8(5)	89.8(3)	13.8(9)
0.30	88.2(2)	9.0(5)	9.6(3)	88.15(20)	89.8(2)	9.0(3)	1.60(5)	12.80	88.2(5)	89.6(3)	10.5(8)
0.60	86.4(2)	8.9(4)	8.7(3)	86.30(20)	89.2(2)	8.9(3)	1.65(5)	13.04	86.6(5)	89.0(4)	11.7(8)
1.00	84.6(3)	9.0(4)	9.1(3)	84.55(20)	88.4(3)	9.1(3)	1.65(5)	13.37	84.8(6)	88.3(4)	12.6(8)

B. Glass scaling of I-V curves with extended and restricted electric-field ranges

Using the ansatz of Eq. (1) one can also determine T_g and z as well as ν for a given set of isotherms via a scaling analysis of the CVC's.^{5-8,12,16} In addition to excluding the high electric-field region of free flux flow, one must also exclude the isotherms above T^* , where the TAFF assumption of Eq. (3) is no longer valid (indicated by dashed lines in Fig. 2). By optimizing the choice of T_g , T^* , z , and ν one can then obtain a collapse of all remaining I-V curves onto the two universal branches. Figure 3 shows excellent scaling for the CVC's at $\mu_0 H = 1.0$ T with $T_g = 84.55$ K, $z = 9.1$, $\nu = 1.65$, and $T^* = 88.4$ K. For all magnetic fields these results agree very well with the analysis of the crossover current and I-V glass line.

The scaling analyses of transport measurements previously published have produced collapses that also appeared quite good but typically yielded dynamic exponents $z = 4-6$, well below our results. While Wöltgens *et al.* have shown that this glass scaling is very sensitive to the detuning of any single parameter,¹⁶ appropriately adjusting all three parameters can still produce a scaling of apparently equal quality provided the measurement window is small enough. This is illustrated in Fig. 4, where the CVC's from Fig. 2 are scaled with a different set of parameters $T'_g = 85.65$, $z' = 6.1$, $\nu' = 1.5$. For a restricted electric-field range with $E > 10^{-5}$ V/m (dots), typical for the majority of previous works, this scaling ($z' = 6.1$) is of the same quality as Fig. 3

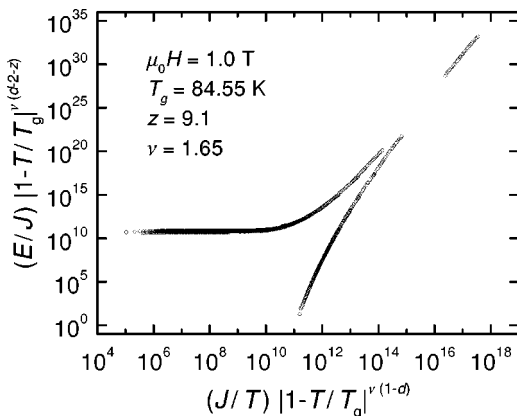


FIG. 3. Glass scaling of the data from Fig. 2 with $T_g = 84.55$, $z = 9.1$, $\nu = 1.65$. Dashed lines in Fig. 2 indicate the range of electric field used in this scaling. Excellent scaling is achieved for the entire accessible electric field, ranging from 10^{-1} V/m to below 10^{-8} V/m.

($z = 9.1$). Therefore the scaling in a reduced electric-field range cannot be deemed conclusive as considerably different sets of parameters yield comparable data collapses. However, the extended electric-field window for this parameter set (triangles in Fig. 4) reveals clear deviations from an acceptable scaling which are due to the Ohmic behavior below J_0^+ for $T_g < T < T'_g$ and appear only at $E < 10^{-5}$ V/m. One should note that this does not imply that the dynamic exponent changes with the electric-field strength. Extending the electric-field range simply leads to a narrowing of the interval of suitable parameters. An acceptable scaling over the full electric-field range is achieved only with the increased dynamic exponent $z \approx 9 \pm 0.5$.

C. Vogel-Fulcher analysis of the resistive transitions

In order to confirm these results we also used a Vogel-Fulcher analysis of resistive transitions $\rho(T, \mu_0 H)$. According to Eq. (3), plotting $\rho(T)$ for a fixed magnetic field as $[d \ln(\rho)/dT]^{-1}$ vs T will result in a linear section for $T^* > T > T_g$. Its slope $\nu(z-1)$ allows the extraction of the product of the critical exponents; its extrapolated temperature intercept corresponds to T_g ; and the deviation of the data from the linear behavior at high temperatures signifies the onset of free flux flow at T^* . Within the experimental uncertainty, the extracted values for T_g and T^* fully agree with those obtained from the analysis of the CVC's. The critical exponents, $\nu(z-1) = 12 \pm 2$, also support a value of $z > 6$ rather than $4 \leq z \leq 6$.

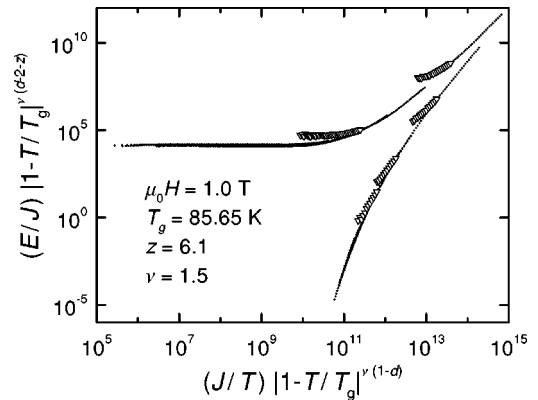


FIG. 4. Scaling of the data of Fig. 2 with a different set of scaling parameters, $T'_g = 85.65$, $\nu' = 1.5$, and $z' = 6.1$. Solid dots represent good scaling comparable to that of Fig. 3 achieved only for data with $E > 10^{-5}$ V/m. Including the low electric-field data (triangles, $10^{-5} > E > 10^{-8}$ V/m) destroys the scaling for these parameters.

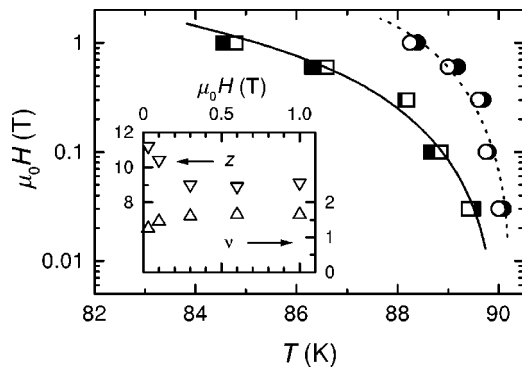


FIG. 5. B - T phase diagram with glass line (squares) and fluid line T^* (circles) as determined from critical scaling (open symbols) and Vogel-Fulcher (solid symbols) analyses. The solid line is a fit to $H_g(T) = H_0(1 - T_g/T_c)^{1.5}$; the dotted line is a guide to the eye. The inset reveals a magnetic field dependence of z and ν below 0.3 T.

V. DISCUSSION

Based on the agreement of all data with predicted qualitative behavior we infer to observe a second-order transition from a fluid to a glassy state. The resulting phase diagram (Fig. 5), in particular the observed glass line $H_g(T)$, gives further support to this notion, as the magnetic-field dependence of T_g is well described by $H_g = H_0(1 - T_g/T_c)^{1.5}$, where $\mu_0 H_0 = 83.5$ T, in agreement with previous results.¹⁷ Also, the onset of the visible magnetic-field dependence of the critical exponents appears at a higher field (0.3 T) but is in general agreement with a reported increase of z at low magnetic fields ($\mu_0 H \leq 0.05$ T) in YBCO.⁶ The most important aspect of our data is, without doubt, the excellent agreement of all analyses establishing a glass transition with a dynamic exponent $z \geq 9$ in the entire magnetic-field range. This value of z clearly exceeds previously reported values of transport measurements (typically 4–6) but one should note that these can be explained within our analysis because the increased z can be unambiguously identified only at very low electric fields. While our $z=9$ only exceeds the original quantitative theoretical predictions of FFH (4–7), alternative explanations other than a VG transition with a high dynamic exponent fail to account for the qualitative observations.

Finite-size effects with $z > 6$ and decreasing T_g have been observed only for strip widths $w < 2 \mu\text{m}^5$ and film thicknesses $t \leq 400$ nm.^{8,16,18} In particular, $z \geq 8$ was found only for $t < 20$ nm.⁸ The dimensions of our samples, $w = 50 \mu\text{m}$ and $t = 400$ nm, are clearly outside the reported limits for finite-size effects. More importantly, in the presence of finite-size effects the (isotropic) glass scaling has failed or a two-dimensional (2D)-3D crossover current, which increases with decreasing temperature, appeared instead of $J_0^+ \propto (T - T_g)^{\nu(d-1)}$. Our results, on the contrary, show excellent

scaling, J_0^+ follows precisely the predicted VG behavior throughout the full experimental window, and the slope of $E_0^+(J_0^+)$ agrees very well with the independent analyses of the I - V glass line and scaling, thus excluding finite-size effects as the cause of the overall increase of z .

With respect to correlated defects the possibility of a Bose glass in YBCO has been suggested,¹⁹ which could present an explanation for deviating critical exponents. However, a Bose scaling on our data results in an even higher dynamic exponent $z_{BG} \approx 14$ instead of $z_{VG} \approx 9$ (also $\nu_{BG} \approx 1$ while $\nu_{VG} \approx 1.6$) which does not render this interpretation more plausible. Also, the model of flux creep (FC), which precludes the existence of a finite temperature $T > 0$ with vanishing linear resistivity, has been applied in the analysis of CVC's.^{11,20} In magnetization measurements of YBCO an observed deviation from the general glassy behavior has been attributed to FC.¹⁰ While we cannot exclude that CVC's may display such features at electric fields below the range of our experiment, this model is an inappropriate explanation for the large dynamic exponent since a static exponent $\nu_{FC} \leq 0.7$ was reported^{10,11} in clear disagreement with our results. Moreover, flux creep cannot account for the excellent scaling nor for the vortex glasslike behavior of the crossover current throughout the entire measurement window.

VI. SUMMARY

In conclusion, we achieved excellent scaling of the CVC's according to the VG theory over a range of more than six decades in the electric field with a transport measurement window extending down to 10^{-8} V/m allowing us to extract T_g , T^* , and the critical exponents. These results are in agreement with the analysis of the resistive transitions and the crossover current J_0^+ . Yet, all results yield a critical dynamic exponent, $z \geq 9$, that is larger than those previously reported (4–6) and predicted by FFH (4–7) throughout the entire investigated magnetic field range (0.03–1.0 T). In the present framework we can exclude finite-size effects and flux creep as the origin of a high value of z . The onset of the observed magnetic-field dependence of the exponents also appears at a somewhat higher value of $\mu_0 H = 0.3$ T but qualitatively agrees with prior reports. Finally, previous scaling analyses that extracted dynamic exponents $z \leq 6$ from CVC's do not actually contradict our findings. If the analysis on our data is restricted to a comparable electric-field range we recover similar results: The evidence for an increased z directly results from the extended electric-field window due to the very long measurement bridge.

The authors wish to thank M. Basset for experimental assistance. Financial support by the Deutsche Forschungsgemeinschaft through Sonderforschungsbereich 262 is gratefully acknowledged.

¹M.P.A. Fisher, Phys. Rev. Lett. **62**, 1415 (1989).

²D.S. Fisher, M.P.A. Fisher, and D.A. Huse, Phys. Rev. B **43**, 130 (1991).

³R.H. Koch, V. Foglietti, W.J. Gallagher, G. Koren, A. Gupta, and M.P.A. Fisher, Phys. Rev. Lett. **63**, 1511 (1989).

⁴C. Dekker, W. Eidelloth, and R.H. Koch, Phys. Rev. Lett. **68**, 3347 (1992).

⁵Y. Ando, H. Kubota, and S. Tanaka, Phys. Rev. Lett. **69**, 2851 (1992).

⁶J.M. Roberts, B. Brown, B.A. Hermann, and J. Tate, Phys. Rev. B

- 49, 6890 (1994); T. Nojima, A. Kakinuma, and Y. Kuwasawa, *Physica C* **263**, 424 (1996).
- ⁷L. Hou, J. Deak, P. Metcalf, and M. McElfresh, *Phys. Rev. B* **55**, 11 806 (1997).
- ⁸A. Sawa, H. Yamasaki, Y. Mawatari, H. Obara, M. Umeda, and S. Kosaka, *Phys. Rev. B* **58**, 2868 (1998).
- ⁹M. Charalambous, R.H. Koch, T. Masselink, T. Doany, C. Feild, and F. Holtzberg, *Phys. Rev. Lett.* **75**, 2578 (1995), and references therein.
- ¹⁰H.H. Wen, X.X. Yao, R.L. Wang, H.C. Li, S.Q. Guo, and Z.X. Zhao, *Physica C* **282-287**, 351 (1997).
- ¹¹S.N. Coppersmith, M. Inui, and P. Littlewood, *Phys. Rev. Lett.* **64**, 2585 (1990).
- ¹²R.H. Koch, V. Foglietti, and M.P.A. Fisher, *Phys. Rev. Lett.* **64**, 2586 (1990).
- ¹³G. Blatter, M.V. Feigel'man, V.B. Geshkenbein, A.I. Larkin, and V.M. Vinokur, *Rev. Mod. Phys.* **66**, 1125 (1994).
- ¹⁴L.F. Cohen and H.J. Jensen, *Rep. Prog. Phys.* **60**, 1581 (1997).
- ¹⁵J. Deak, M.J. Darwin, and M. McElfresh, *Physica A* **200**, 332 (1993); D.G. Xenikos, J.T. Kim, and T.R. Lemberger, *Phys. Rev. B* **48**, 7742 (1993).
- ¹⁶P.J.M. Wöltgens, C. Dekker, R.H. Koch, B.W. Hussey, and A. Gupta, *Phys. Rev. B* **52**, 4536 (1995).
- ¹⁷J. Kötzler, M. Kaufmann, G. Nakielski, R. Behr, and W. Assmus, *Phys. Rev. Lett.* **72**, 2081 (1994); J. Kötzler, G. Nakielski, M. Baumann, R. Behr, F. Goerke, and E.H. Brandt, *Phys. Rev. B* **50**, 3384 (1994).
- ¹⁸C. Dekker, P.J.M. Wöltgens, R.H. Koch, B.W. Hussey, and A. Gupta, *Phys. Rev. Lett.* **69**, 2717 (1992).
- ¹⁹P.J.M. Wöltgens, C. Dekker, J. Swüste, and H.W. de Wijn, *Phys. Rev. B* **48**, 16 826 (1993).
- ²⁰R. Griessen, *Phys. Rev. Lett.* **64**, 1674 (1990).